

Time-dependent local-density approximation in real time

K. Yabana

Department of Physics, Niigata University, Niigata, Japan

G. F. Bertsch

Physics Department and Institute for Nuclear Theory, University of Washington, Seattle, Washington 98195

(Received 24 January 1996)

We study the dipole response of atomic clusters by solving the equations of the time-dependent local-density approximation in real time. The method appears to be more efficient than matrix or Green's function methods for large clusters modeled with realistic ionic pseudopotentials. As applications of the method, we exhibit results for sodium and lithium clusters and for C_{60} molecules. The calculated Mie resonance in Na_{147} is practically identical to that obtained in the jellium approximation, leaving the origin of the redshift unresolved. The pseudopotential effects are strong in lithium and act to broaden the Mie resonance and give it a substantial redshift, confirming earlier studies. There is also a large broadening due to Landau damping in the calculated C_{60} response, again confirming earlier studies. [S0163-1829(96)02631-8]

The time-dependent local-density approximation (TDLDA) has been widely applied to the collective electronic excitations of atomic clusters, starting with jellium calculations by Ekardt.¹ The usual formalism is based on linear response with frequency rather than time as a variable. The resulting Green's function equations may be solved directly in coordinate space¹⁻⁴ or in a particle-hole configurational representation.⁵⁻⁷ The direct coordinate-space method is very efficient when the system has spherical symmetry, reducing the integral equation to a one-dimensional equation. However, realistic theory requires that the ion cores be treated explicitly, losing the spherical symmetry. Then the Green's function method requires a matrix representation of operators on in three-dimensional space, which makes the overall dimensionality too large to handle. The configurational representation, on the other hand, is limited by the dimensionality of the particle-hole space. This depends on the number of particles in the system calculated; for moderate numbers of particles in three dimensions it is more practical than the other methods.

We think that the most effective method for large numbers of particles in three dimensions is to go back to the time representation and explicitly calculate the time evolution of the initial configuration. Since only a single Slater determinant is evolved, one does not get into the multiplicity problem of the particle-hole representation. And because the Hamiltonian matrix is rather sparse in a coordinate-space representation, one avoids the very large matrix dimensionality problem of the Green's function method.

We shall illustrate the method with several examples, taken from alkali metal clusters and C_{60} molecules. Our pseudopotentials are constructed following the method of Troullier and Martins.⁸ We first calculate local pseudopotentials in the s and p waves defined to produce pseudo-wavefunctions that match the Hartree-Fock wave functions smoothly at a certain radius r_c . The pseudopotential in the Hamiltonian has two parts, a local potential identical to the p -wave pseudopotential, and a separable nonlocal potential

that acts in the s wave and accounts for the difference in the s and p wave interactions. The nonlocal part is determined by the method of Kleinman and Bylander.⁹ The electron-electron interaction is treated as is commonly done, taking into account exchange and correlation effects with the contact interaction from Perdew and Zunger.¹⁰ As a first step, we must find the ground state electronic configuration. We shall assume that the ionic geometry is known and so we only have to solve the Kohn-Sham equation for the electrons. This is done with the same representation of the Hamiltonian as will be used for the response. Given the electron wave functions for the ground state, we next perturb them by the replacement

$$\phi' = e^{ikz}\phi.$$

This gives the electrons a coherent velocity field and causes a dipole moment to develop as the system evolves with time. We solve the time-dependent equations of motion, keeping track of the dipole moment. The Fourier transform of the dipole moment is the response that we seek. The wave number k must be much smaller than the inverse radius of the system for the response to be dipolar and linear in the perturbing field.

We now discuss some of the numerical details. It is important to have high-order algorithms to evaluate the kinetic energy operator and integrate the time-dependent Kohn-Sham equation. We use algorithms that have proved successful in nuclear physics¹¹ and have also been successful in solving the Kohn-Sham equation.¹⁵ We use the nine-point difference formula to evaluate the Laplacian operator (called $N=4$ in Ref. 15). The time-dependent Kohn-Sham equation is integrated with a fourth-order Taylor expansion of the TDLDA equation. In this expansion, the electron density is fixed to evaluations at times half way between the wavefunction evaluations by a predictor-corrector method. This

TABLE I. Numerical parameters in the TDLDA calculations.

System	Δx (\AA)	R (\AA)	N	$\Delta t/\hbar$ (eV^{-1})	N_t
Jellium (Li_{138})	1.5 \AA	15 \AA	4169	0.01 eV^{-1}	5000
Li_{147}	0.8	15	27609	0.01	5000
Na_{147}	0.8	15	27609	0.01	5000
C_{60}	0.3	6.5	42691	0.001	5000

prescription has been shown to conserve energy to a high accuracy.¹¹ The additional numerical quantities that need to be specified are the mesh spacings, the size of the box in which the wave function is calculated, and the number of mesh points. For our purposes here, calculating only the electronic properties at a fixed ionic geometry, convergence can be obtained with rather coarse meshes. We use a spherical box of radius R to truncate the Cartesian lattice of mesh points. The values we used are shown in Table I. As one might expect, the alkali metals can be treated with much coarser meshes than elements like carbon that form much more compact structures.

Before presenting the results of the calculations with ionic pseudopotentials, we show how the method compares with the Green's function technique for the jellium calculation. We assume a jellium sphere with a density parameter $r_s = 3.25$ a.u. and a radius of 8.88 \AA , corresponding to a cluster of 138 lithium atoms, Li_{138} . Figure 1 shows the RPA result calculated with the Green's function method as well as the Fourier transform of the response calculated from the time evolution of the Hamiltonian. The response is expressed in units of the single-electron sum rule per eV; thus the integrated response gives the number of valence electrons. The RPA calculation was done in a spherical basis, while the TDLDA calculation was done in a three-dimensional mesh as described above. For both calculations, the response has been smoothed out by adding a small imaginary part to the frequency (0.05 eV). For the TDLDA computation, this is done by including a damping factor $\exp(-\gamma t)$ in the integrand of the Fourier transform. The only difference one sees

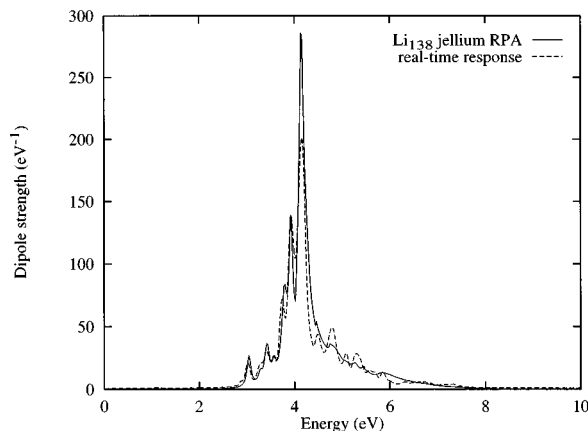


FIG. 1. Dipole response of a jellium sphere corresponding to the cluster Li_{138} . The solid line shows the RPA calculation using a spherical Green's function representation, and the dashed line shows the result of real-time integration of the TDLDA equations on a three-dimensional coordinate-space mesh.

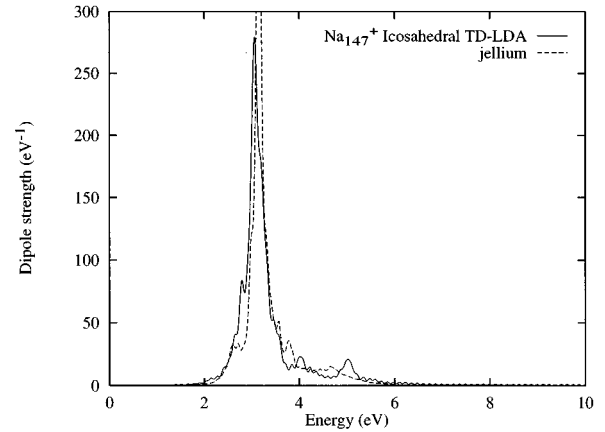


FIG. 2. Comparison of jellium and pseudopotential Hamiltonians for the response of the sodium cluster Na_{147}^+ . The dashed line shows the jellium calculation at a density $r_s = 3.93$ and the solid line is the pseudopotential result.

between the two methods in Fig. 1 is the greater structure in the TDLDA response above the ionization threshold. This is a consequence of the finite box size in the TDLDA algorithm; the Green's function method treats the electron continuum explicitly.

We now examine some individual systems with the full pseudopotential treatment. We start with sodium, which has a rather weak pseudopotential. We consider the 147 atom cluster arranged as a Mackey icosahedron. There is some evidence¹² that the ionization potentials of alkali metal clusters have a periodicity corresponding to the Mackey icosahedra. We took the nearest-neighbor distance between atoms in adjacent layers to be 3.66 \AA , corresponding to nearest-neighbor spacing in the bulk metal (bcc lattice). The response is shown in Fig. 2, compared with the jellium model. The peak at 3.0 eV agrees well with the jellium model. This is not surprising; the pseudopotential for sodium is quite weak and has a very small momentum dependence. The position of the resonance is about 15% higher than the empirically observed Mie resonance, leaving this long-standing discrepancy between theory and experiment unresolved. Of course, the geometry may well be more diffuse than we have assumed, perhaps due to thermal motion.

The Mie resonance in Li clusters has the largest redshift of any alkali metal clusters, making this system especially interesting to gain a fundamental understanding of the redshifts. We again assume an icosahedral structure. Here, the spacing between layers is taken as 3.02 \AA , corresponding as before to the nearest-neighbor distance in the bcc bulk structure. It is also of interest to see whether the high symmetry of the icosahedron has an effect on the shape of the Mie resonance, and so we have also calculated the response assuming a different geometric structure for the cluster. It is possible to enclose exactly 147 atoms in a sphere on an fcc lattice, and we calculated this case as well. In Fig. 3, we compare the pseudopotential-LDA calculation with experiment for both structures. The fcc response is slightly broader than the icosahedral. In both cases the theory is redshifted almost to the full amount required by the experiment. This redshift is due to the state dependence of the pseudopotential. We have verified this by repeating the calculation with a state inde-

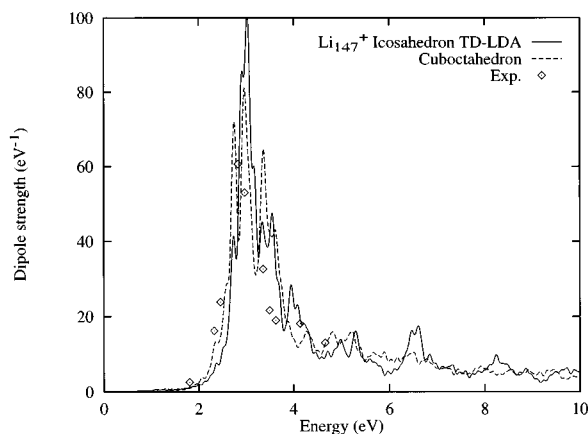


FIG. 3. Pseudopotential calculations for lithium cluster response, with two different models for the ionic geometry. The dashed line shows Li_{147}^+ with a spherically truncated fcc structure, and the solid line shows Li_{147}^+ with a Mackey icosahedral structure. Data points are from Ref. 18.

pendent potential, using the s -state pseudopotential in all partial waves. Then the Mie resonance peaks at about 4 eV instead of at 3 eV, close to the jellium position. The importance of the nonlocality of the pseudopotential for the redshift has been discussed earlier, using more simplified treatments of the Hamiltonian.^{7,13,14} In Refs. 7 and 13 the pseudopotential was spherically averaged in the Hamiltonian, losing the discreteness of the ionic structure. In our own previous work, Ref. 14, we used contact pseudopotentials, which also exhibit the qualitative effects associated with nonlocality. While contact potentials are very convenient to work with, they are of unproven reliability, and we shall see, in the next example, that they can give misleading results. It should also be mentioned that Ref. 14 also used a separable form for the time-dependent electron-electron interaction, which tends to give more collectivity to the Mie resonance than more refined treatments of the interaction.

For completeness in the presentation of the real-time method for solving TDLDA, we show in Fig. 4 the real-time response of Li_{147}^+ . The dipole moment is plotted as a function of time.

Our final example is the response function for C_{60} , shown in Fig. 5. The valence space for carbon includes the

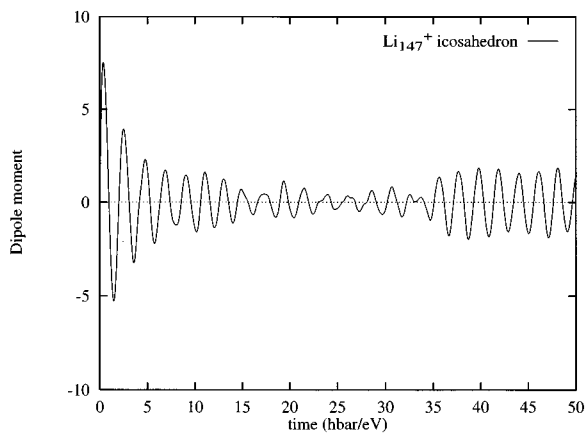


FIG. 4. Time dependence of dipole moment in Li_{147}^+ .

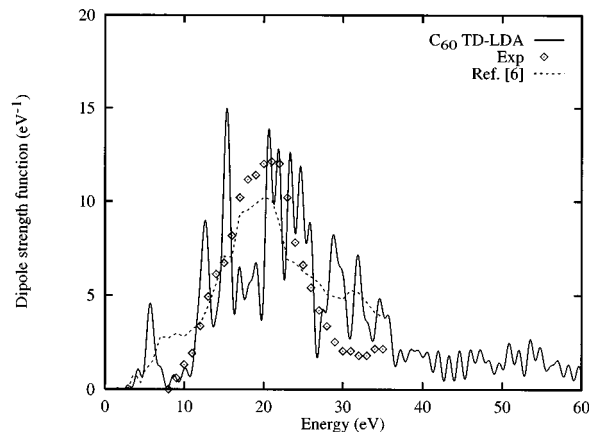


FIG. 5. Response for C_{60} with the pseudopotential-LDA Hamiltonian. The diamonds show the photoionization data of Ref. 19, which has an arbitrary normalization. The dashed curve is the TDLDA calculation of Ref. 6.

four electrons in the s and p orbitals, and the energy spread of the single particle states is much larger than in the alkali metals. For this system we had to use a mesh spacing of 0.3 Å to get a good convergence of the electronic calculation. The required time step is also much smaller, due to the higher frequency range of the response. We evolved the system for a shorter time, so the energy resolution is poorer on an absolute scale than for the previous examples. The main features of the calculated response function are the small peak at 7 eV, representing mainly π electron excitations, and the much larger broad structure between 15 and 25 eV, representing σ electron excitations. The sum rule strength in the π electron peak, obtained by integrating over energies in the range 2–10 eV, is 9 (out of 240 total, if the pseudopotential were local). Experimentally, there are several peaks, particularly at 4.8 and 5.9 eV and the measured strength up to 7 eV is 6.¹⁶ The calculation thus gives a reasonable strength in this region, although it misses the detailed structure. The σ plasmon is very much broadened in the pseudopotential-based TDLDA, whereas in simplified tight-binding models, it is much narrower.¹⁷ Our results are similar to those of Ref. 6, who calculated the pseudopotential-TDLDA response in a frequency- and configuration-space representation. In a previous work,²⁰ we calculated the C_{60} response using a contact pseudopotential, which produced a broad distribution of strength extending up to 60 eV. The strength at high energy thus appears to be an artifact of the contact pseudopotential.

Another quantity of interest in C_{60} is its polarizability. This may be extracted from the response S using the formula

$$\alpha = \frac{e^2}{m} \int \frac{S(E) dE}{E^2},$$

where S is normalized according to the sum rule $\int S dE = N_e$. Our calculated polarizability is $\alpha = 80 \text{ \AA}^3$, in good agreement with the value 85 \AA^3 that may be obtained from the dielectric constant $\epsilon \approx 4$. Here, the tight-binding model is rather far off, predicting $\alpha \approx 45 \text{ \AA}^3$.

This work was initiated at the Institute for Nuclear Theory, and is supported by the Department of Energy under Grant No. DE-FG06-90ER40561, and by a Grant in Aid for Scientific Research

(No. 07740250) of the Ministry of Education, Science and Culture (Japan). Numerical calculations were performed on the FACOM VPP-500 supercomputer in RIKEN.

-
- ¹W. Ekardt, Phys. Rev. Lett. **52**, 1925 (1984); Phys. Rev. B **31**, 6360 (1985).
²D.E. Beck, Phys. Rev. B **35**, 7325 (1987).
³S. Saito *et al.*, Phys. Rev. B **42**, 7391 (1990).
⁴M.J. Puska, R.M. Nieminen, and M. Manninen, Phys. Rev. B **31**, 3486 (1985).
⁵C. Guet and W.R. Johnson, Phys. Rev. B **45**, 11 283 (1992); M. Madjet, C. Guet, and W.R. Johnson, Phys. Rev. A **51**, 1327 (1995).
⁶C. Yannouleas, E. Vigezzi, and R.A. Broglia, Phys. Rev. B **47**, 9849 (1993); F. Alasia *et al.*, J. Phys. B **27**, L643 (1994).
⁷L. Serra *et al.*, Phys. Rev. B **48**, 14 708 (1993).
⁸N. Troullier and J.L. Martins, Phys. Rev. B **43**, 1993 (1991).
⁹L. Kleinman and D. Bylander, Phys. Rev. Lett. **48**, 1425 (1982).
¹⁰J. Perdew and A. Zunger, Phys. Rev. B **23**, 5048 (1981).
¹¹H. Flocard, S. Koonin, and M. Weiss, Phys. Rev. C **17**, 1682 (1978).
¹²T.P. Martin, T. Bergmann, H. Gohlich, and T. Lange, Z. Phys. D **19**, 25 (1991).
¹³S. Blundell and C. Guet, Z. Phys. D **33**, 153 (1995).
¹⁴K. Yabana and G.F. Bertsch, Z. Phys. D **32**, 329 (1995).
¹⁵J. Chelikowsky, N. Troullier, K. Wu, and Y. Saad, Phys. Rev. B **50**, 11 355 (1994).
¹⁶S. Leach *et al.*, Chem. Phys. **160**, 451 (1992).
¹⁷G. Bertsch, A. Bulgac, D. Tomanek, and Y. Wang, Phys. Rev. Lett. **67**, 2690 (1991).
¹⁸C. Brechignac *et al.*, Phys. Rev. Lett. **70**, 2036 (1993).
¹⁹I.V. Hertel *et al.*, Phys. Rev. Lett. **68**, 784 (1992).
²⁰K. Yabana and G.F. Bertsch, Phys. Scr. **48**, 633 (1993).